

Convection during the vertical Bridgman growth of $\text{Hg}_{1-x}\text{Cd}_x\text{Te}$

V. FANO, I. ORTALLI, K. POZELA, G. MELETTI
Physical Science Institute, University of Parma, 43100 Italy
Maspec Institute of CNR, Parma, 43100 Italy

Two different structures, obtained with specific growth parameters, in $\text{Hg}_{1-x}\text{Cd}_x\text{Te}$ single crystals synthesized by the vertical Bridgman technique, are shown. A structure (small vertical line-shaped defects) located in the central part of the charge along the growth axis can be ascribed to convection induced by melt–solid interface curvature. The other structure, obtained in the first-to-freeze region of the ingot, when the temperature of the cold zone of the furnace is constant and a few degrees lower than the solidification one, can be ascribed to the convection rolls frozen in the solid matrix. © 1998 Chapman & Hall

1. Introduction

Recently some attempts have been made to detect natural convection during crystal growth of semiconductors for the better understanding of the role played by convection in the variation of physical properties. On this matter experiments under different gravity conditions have been carried out using the unidirectional crystal growth from the melt by the Bridgman method, producing crystals with a more homogeneous axial composition in low gravity conditions. This can be explained by the change from the convective growth on earth to the diffusion-controlled steady-state growth in space. Additional information has been obtained by experiments on the Bridgman growth of $\text{Pb}_{0.8}\text{Sn}_{0.2}\text{Te}$ in high gravity conditions [1–3]. In order to show the influence of other parameters inducing convection, experiments on the melt–solid interface shape have been undertaken. This is an important processing parameter in Bridgman crystal growth [4–6]. The interface shape and position are controlled by a combination of material properties, ampoule characteristics and thermal conditions in the furnace [7–14]. Specific techniques have been used to determine interface location and shape [15–19]. A flat shape, which is difficult to obtain, is compatible with purely diffusive solute transport in the melt. Thus, in the most cases, the mixing by thermal and/or solutal convection must be expected. Generally, a flat shape or a slightly convex (with respect to the solid) interface is desirable in order to limit both spurious nucleation on the walls of the ampoule and low-angle grain boundaries in Bridgman-grown crystals. Numerical experiments [20] have suggested that the dimensionless interface temperature can be an important controlling parameter in adjusting the interface shape in vertical Bridgman growth. For semiconductors, having thermal conductivity of the melt greater than that of the solid, the melt is cooled by the ampoule. As a result the solidification isotherms are distorted [9, 16, 21, 22], producing thus

a concave growth interface. The real shape of a solid–melt $\text{Hg}_{1-x}\text{Cd}_x\text{Te}$ interface has been obtained by quenching the ampoule during the Bridgman growth of crystals [16] or while growing under conditions of accelerated ampoule rotation [23]. In the last case, the variation of the rotation speed affected the interface shape. It has been reported [24, 25] that in $\text{Pb}_{1-x}\text{Sn}_x\text{Te}$ grown by the vertical Bridgman technique the diffusionless melt–solid transformation occurs in the supercooled melt at the onset of the solidification process, and the length of this uncontrolled growth (very fast velocity growth) is inversely related to the temperature gradient of the furnace. It seems also that the convective driving forces are sufficiently strong to exchange material from the first-to-cool capillary-shaped region with the bulk volume in the early stage of the growth.

The mixing of the melt by convection has been demonstrated also by the distribution of the components along the length of the ingot [19, 25]; however, no data are available now concerning a direct view of the convective motion and its intensity. The attempt to see the convective motion by quenching the melt inevitably results in a dendritic structure with primary dendritic arm spacing depending on the local solidification time or the thermal gradient and growth rate. In this work we show specific crystal structures that can be ascribed to the convection movements. Mercury cadmium telluride, with starting composition of 20 mol% CdTe, was selected as a system to study the behaviour of narrow-gap semiconductors, which segregates a high density component (mercury-rich component) at the solid–melt interface, in the vertical Bridgman process. The solidification of this material, used for optoelectronic devices, is interesting because the melt can show convective instability. In fact, the vertical Bridgman configuration will show a radial temperature gradient and solutal gradient, due to Hg rejection, a solid–melt interface that is not planar. The horizontal component of the gravity vector with

respect to the growth axis will produce convective instability and cause movement of the heavy Hg-rich component towards the bottom of curvature. For revealing the structures related to the convective mixing in the boundary layer region, a thermal gradient of about $20^{\circ}\text{C cm}^{-1}$ and a 2 cm h^{-1} growth velocity have been used. These growth conditions are a good compromise that gives a significant thickness to the boundary layer. The growth velocity of 2 cm h^{-1} is relatively high with respect to those generally used, and it produces the wrong interface shape for crystal growth, which increases the horizontal component of the gravity vector. Conversely, higher growth velocities are not advisable, because they give dendritic structures.

As concerns the fluid flow patterns forming convective rolls, these figures were obtained when the solidification process in the Bridgman configuration was carried out at a temperature a little lower (5°C) than the solidification temperature. In these conditions and owing to the mixing by convection, the charge, when lowered, will continue to be melted, even if it is partially located in the cold zone. The solidification, when it starts at the bottom of the ampoule placed in the cold zone of the furnace, will take place in the condition of a small radial thermal gradient and will involve instantaneously a large part of the melt, trapping the convective rolls.

2. Experimental procedure

The $\text{Hg}_{0.8}\text{Cd}_{0.2}\text{Te}$ charges (8 cm length) were prepared by oxygen-free high purity elements in out-gassed quartz ampoules (1.6 cm inner diameter, 2.1 cm outer diameter) with conical tip (2.5 cm height) configuration. The elements reacted in inert gas atmosphere at 830°C for 8 h. Afterwards, the ampoule was sealed off with 10^{-6} mmHg vacuum. Then it was placed in the hot zone of the crystal growth apparatus. The Bridgman apparatus used in this work was a vertical two-zone furnace (see Fig. 1). After thermal equilibration, the ampoule was lowered at constant velocity from the hot zone through a gradient zone. In order to obtain a sharp and relatively deep curvature of the melt-solid interface, we chose 2 cm h^{-1} growth velocity instead of a lower velocity (for instance, 0.5 cm h^{-1}). Two different thermal gradients, schematically reported in Fig. 2 a and b, were used. Gradient a ($20^{\circ}\text{C cm}^{-1}$ at the solid-melt interface) is usually used in $\text{Hg}_{0.8}\text{Cd}_{0.2}\text{Te}$ growth. Making use of these growth conditions, we examined the shape of the interface and the magnitude of the boundary layer. To reveal the interface shape, the growth, carried out with the thermal gradient a, was interrupted at a chosen time and quenched by rapidly pushing the ampoule into the cooling jacket of the furnace.

The gradient b is different from a because the temperature of the cold zone was kept only 5°C below the solidification temperature, which was supposed to be 760°C . The onset of the crystal growth is delayed when the gradient b (instead of a) is used, and we obtain a large volume of the melt in the cold zone of the furnace. In this way a large quantity of the melt

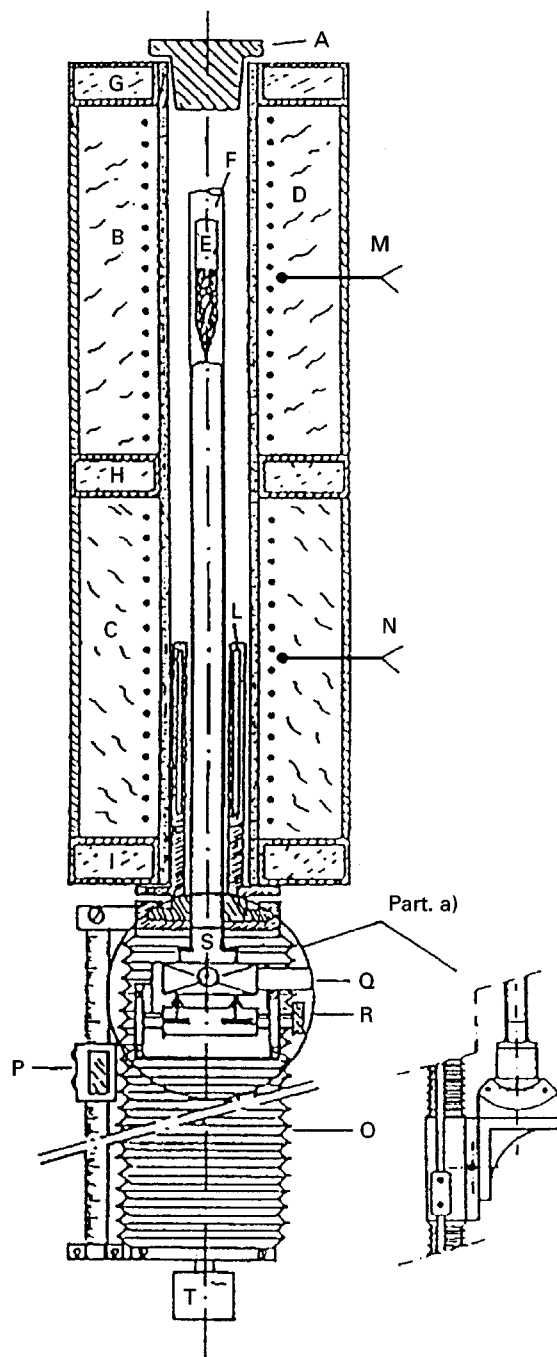


Figure 1 Sketch of two-zone Bridgman apparatus.

takes part in the melt-solidification process at the onset of the growth, making easy the detection of the effects of the convection in the melt by optical microscopy. To study composition variations, X-ray microanalysis was used.

3. Results and discussion

3.1. Interface shape

The interface shape was revealed in charges grown in the thermal gradient a. The growth of the crystals of different lengths was interrupted by quenching and the ingots were removed from the ampoule by breaking the silica tube. The ingots were then cut in half along their length. The interface was visible on the lapped surface, but etching with 2% bromine-methanol solution was used to reveal the details. The quenched melt

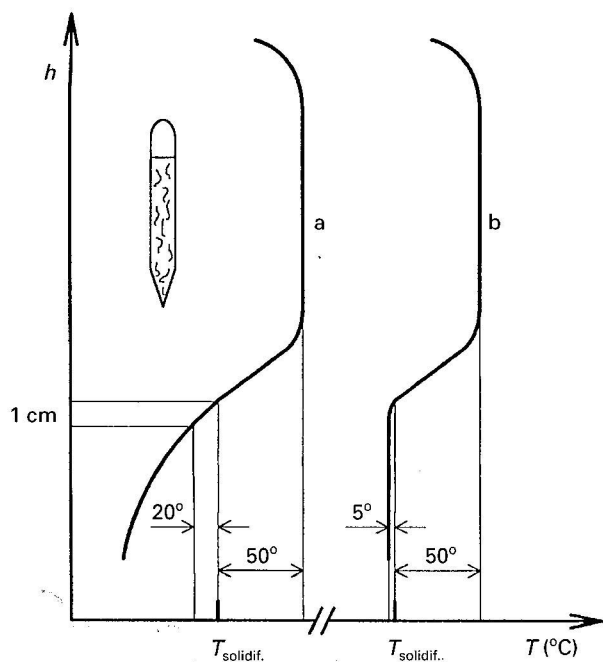


Figure 2 Thermal gradients taken from two Bridgman growth experiments. The difference between gradient a and gradient b is that the temperature profile of a is a gradient generally used in the growth of $\text{Hg}_{1-x}\text{Cd}_x\text{Te}$; b is constant in the cold zone of the furnace with a temperature of few degrees lower than the solidification one.

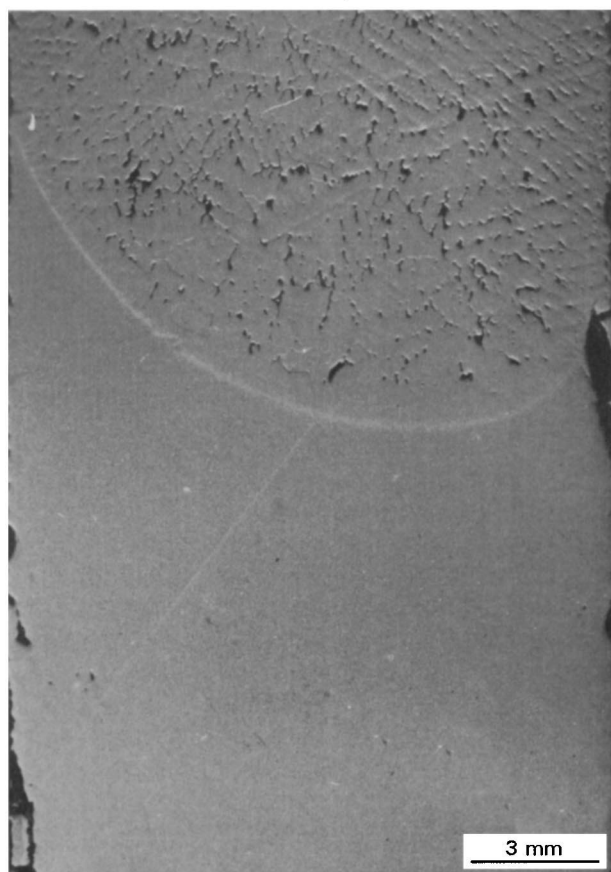


Figure 3 Quenched interface in the etched longitudinal section of $\text{Hg}_{0.8}\text{Cd}_{0.2}\text{Te}$ obtained with the thermal gradient a and growth velocity 2 cm h^{-1} .

phase was characterized by a dendritic structure. The interface shape was asymmetric and concave towards the melt (see Fig. 3). The curvature of the interface was depressed with respect to the two extreme points by

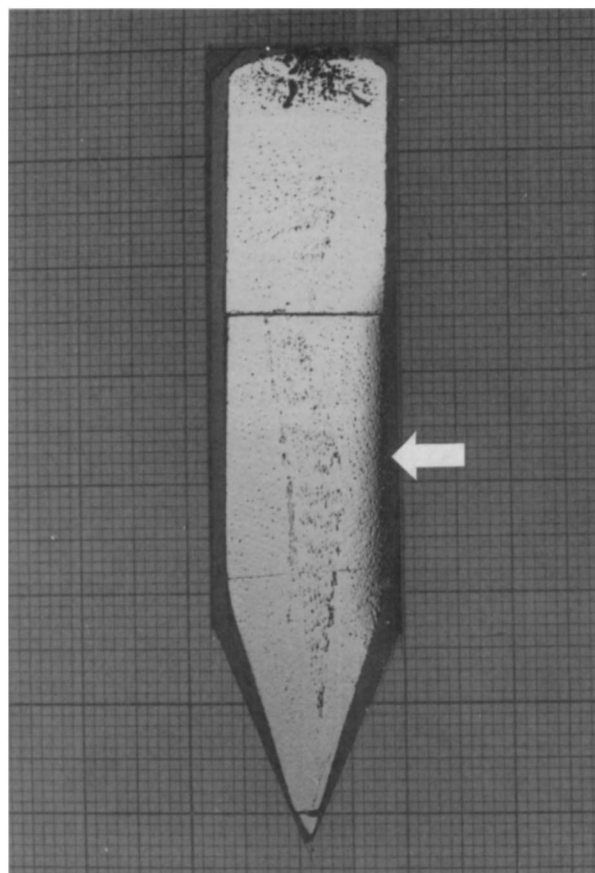


Figure 4 Line-shaped structure along the growth axis of $\text{Hg}_{0.8}\text{Cd}_{0.2}\text{Te}$ section (16 mm width) grown with thermal gradient a and growth velocity 2 cm h^{-1} . The ingot has been sliced into different zones perpendicular to the growth axis for the compositional analysis.

about 7.6 mm and 2.9 mm, respectively. The interface shape was constant for a major part of the growth, indicating that the steady decrease in the ratio of melt to crystal in the ampoule did not cause a significant change in heat transfer. According to Capper *et al.* [16], the line below the actual solid-melt interface, which was clearly visible (see Fig. 3), was ascribed to the boundary layer. The width of this layer changed from about $120\ \mu\text{m}$ (in the upper part of the curvature) to about $270\ \mu\text{m}$ (at the bottom of curvature). These values and the shape of the interface are consistent with mixing driven by convection and their average is in qualitative agreement with the values ($\sim 200\ \mu\text{m}$) reported by Capper *et al.* [16] and with the calculated ones in [25] for an analogous system (lead-tin-telluride). The change in thickness of the layer from 120 to $270\ \mu\text{m}$ can be qualitatively explained by the influence of the gravitational field on the mercury-rich layer. The heavy mercury moves down from the upper part of the curvature, causing thus a density-driven convective flow. This fact seems to be confirmed by the presence of vertical lines (see Fig. 4) in the crystal centre just where the thickness of the Hg-rich boundary layer increases: the line set is shifted from the centre of the ingot exactly as the bottom of the boundary layer is shifted. The supposition is that these lines are due to flow of the low temperature melting (Hg-rich) component, frozen in during the growth. In fact,

the thermoelectric microprobe is much more scattered in this central zone, when compared with uniform side part (see Fig. 5). The behaviour of the curvature is confirmed by the compositional analysis of Hg, Cd, Te reported in Fig. 6, that shows the Hg increase in the central region of the crystal.

3.2. Convective rolls

Fig. 7a–g is referred to the first-to-freeze solid (3 cm length), which includes the conical part (2.5 cm) of a charge grown with gradient b. The photos report samples obtained in succession by slicing the solid into 10 parts (each spaced 3 mm one from another) perpendicularly to the growth axis. The slices were lapped, chemically etched and observed with an optical microscope. The general view of the curved lines, often concentric, seems to be convective flow patterns, i.e. cross-sections of one or two convective rolls frozen-in during the solidification. These figures are absent in

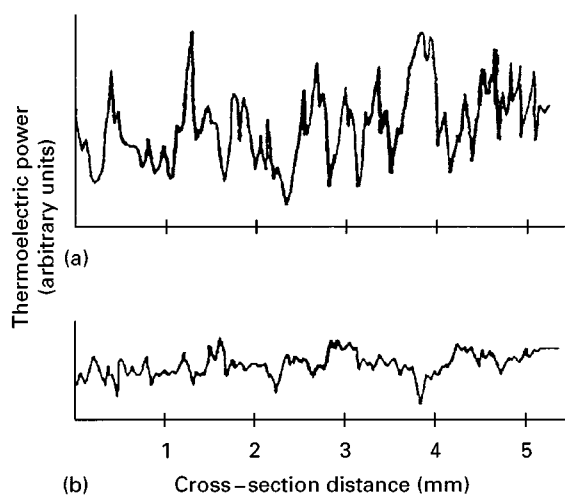


Figure 5 Thermoelectric microprobe test in the central part perpendicular to the growth axis of the crystal reproduced in Fig. 4.(a) the region of line-shaped structure; (b) the adjacent compacted region.

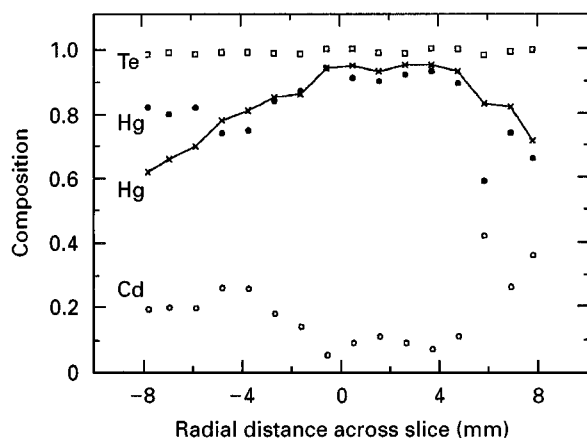


Figure 6 Compositional variations along two radial scans. Continuous fine (×) is Hg in central region of the ingot reported in Fig. 4; (□), (●), (○) are Te, Hg and Cd, respectively, in the slice of Fig. 7g. For simplicity, Cd and Te (the concentration of Te is always 1.0) are omitted for the sample of Fig. 4.

the rest of the charge, suggesting thus that the volume of the solid containing the convective flow patterns solidifies simultaneously in the early stage of solidification owing to the small difference between the furnace temperature and that of the forming solid; this simultaneous solidification would be different from solidification by quenching, which takes place with large thermal gradients. In order to assess the hypothesis of simultaneous solidification we quenched a charge, the movement of which was interrupted when the ampoule tip reached about 2 cm into the cooled zone of the furnace. The length of 2 cm is smaller than that containing the convective flow patterns shown in Fig. 7. The structure of the first 2 cm (conical-shaped) quenched ingot was similar to the rest of the ingot, i.e. it was polycrystalline, dendritic type, without a solid-melt interface at the point of quenching, confirming thus that all the charge was melted before the quenching. Conversely, the curved melt–solid interface was present at about the point of quenching, in all charges, the movements of which were interrupted when the distance covered by the ampoule tip into the cooled zone of the furnace was more than 2 cm. This confirmed that the convective rolls were formed simultaneously. The flow patterns were absent also when the usual gradient (gradient a) was used. In the last case, owing to the major loss of heat from the ampoule tip, the melt volume involved in the simultaneous solidification was small.

The formation of rolls can be based on the following remarks. Let us consider the uniform cooling at the surface of the ampoule part (in our case ~3 cm length) located in the colder zone of the growth apparatus (see Fig. 8, which shows a sketch of this part of the ampoule). This part consists of a vertical wall (the cylindrical part of the ampoule) with a constant depth (from the wall to the axis of the cylinder) and a sloping wall (the conical part of the ampoule) with a changing depth. We take into account that the rate of change of density of a melt layer depends inversely on the depth [26]. By geometrical considerations, the melt at B (see Fig. 8) becomes heavier faster than that at A, owing to a uniform cooling of the ampoule surface. The pressure gradient in the horizontal plane defined by AB drives a circulation as shown in Fig. 8 (a flow down the slope to the bottom). At point C, the melt becomes lighter more slowly than at D. This induces a circulation from C to D. [26]

X-ray microanalysis was carried out to compare the radial composition variation between two slices of different axial position: the slice reported in Fig. 7g (horizontal plane at about 3 cm from the tip) and the slice indicated by an arrow in Fig. 4. The morphology of the structure after chemical etching does not reveal convective rolls (see below) in this last slice. The results of microanalysis are reported in Fig. 6, which shows the data of scans performed along the diameter of the samples. For simplicity the compositional distribution of Te (which is constant) and Cd of the sample, reported in Fig. 4, has been omitted. The Hg distribution in this last sample is less scattered and shows better the parabolic variation in HgTe content from the center to the edge.

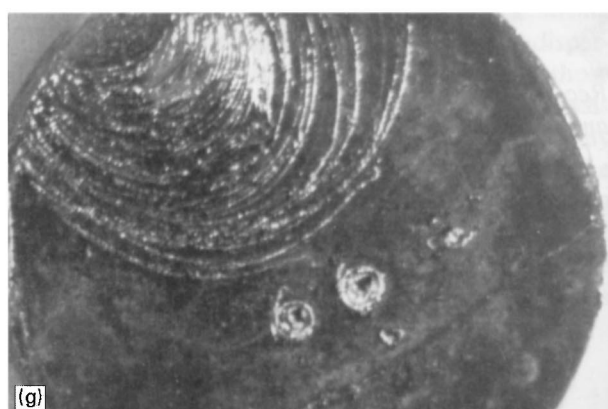
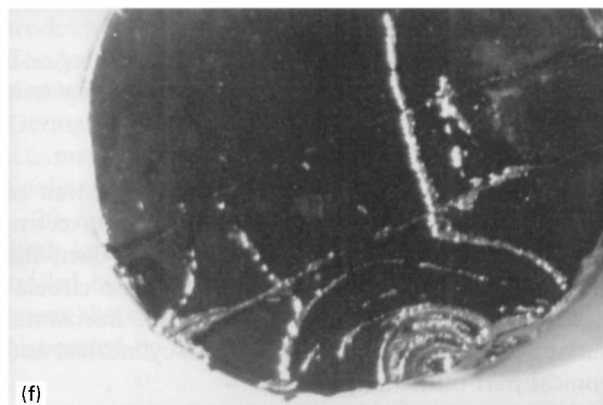
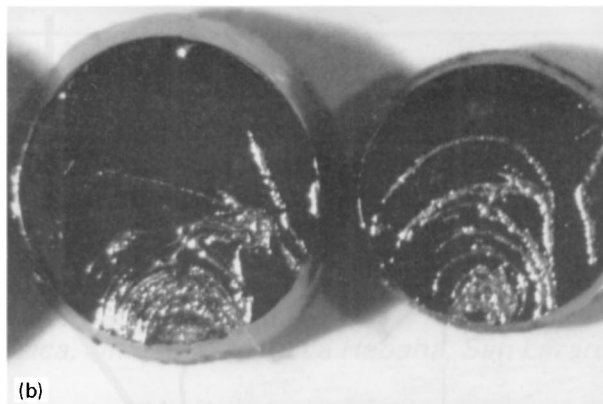
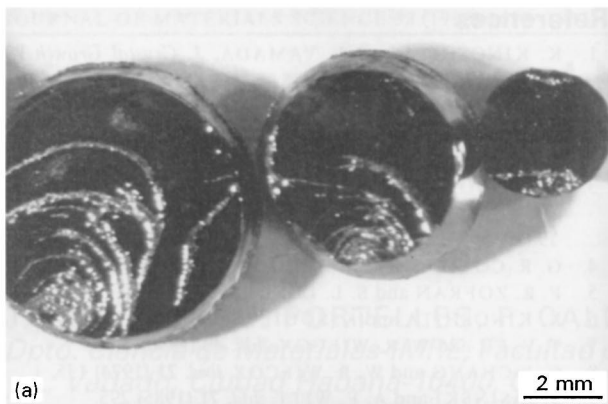


Figure 7 Convective rolls in the first-to-freeze (3 cm) solid. The conical part of the solid is 2.5 cm in height. The slices are spaced 3 mm one from another. The same magnification has been used in all photos.

4. Conclusions

It is difficult to calculate the boundary layer thickness of mercury cadmium telluride in the vertical Bridgman configuration, because several parameter in-

involved in the calculation are not available. But the thickness can be evaluated with the method of detection reported in [23]. The achievement of a sharp curvature (~ 7 mm depth), due to increased growth velocity, gives additional information: the thickness of the boundary layer seems to be large at the bottom of the curvature ($270 \mu\text{m}$) with respect to the extreme points ($120 \mu\text{m}$) because of the motion of the heavy Hg-rich interface layer down towards the bottom. These values are in agreement with the presence of convection movements in the bulk melt. This picture is associated with the presence of vertical lines escaping from the bottom of the curvature, probably due to the highly volatile Hg-rich component. The compositional dishomogeneity in the region of the vertical lines is confirmed by the behaviour of thermoelectric microprobe.

A direct detection of convective rolls, developed in the bulk melt, can be seen when a constant temperature, whose value is few degrees lower than the solidification one, is used in the cold zone of the growth apparatus. In this case the radial temperature gradient

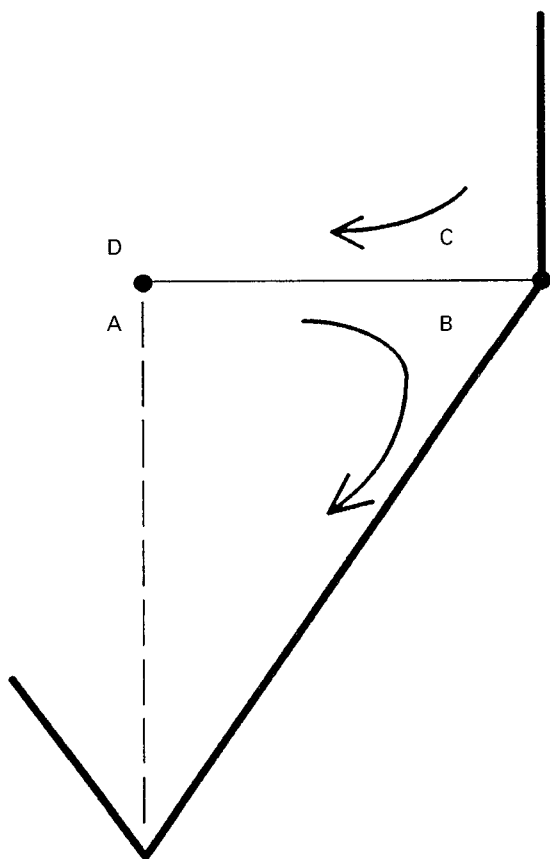


Figure 8 Sketch of the melt flows produced in the lower region of the ampoule with sloping walls, when the cooling temperature is constant.

is minimized and the simultaneous solidification of a large amount of the melt freezes-in the convective rolls in the first-to-freeze ingot region. In fact, the sloping boundary of the container can cause circulations driven by a flux imposed over the horizontal surface of the basal plane between the cylindrical and conical part of the ampoule.

Acknowledgement

One of the authors (K. Pozela) undertook this work with the support of the ICTP Programme for Training and Research in Italian Laboratories, Trieste, Italy.

References

1. K. KINOSHITA and T. YAMADA, *J. Crystal Growth* **99** (1990) 1276.
2. L. L. REGAL, A. M. TURCHANIMOV, O. V. SHUMAEV, I. N. BANDEIRA, C. Y. AN and P. H. O. RAPPL, *ibid.* **119** (1992) 94.
3. H. RODOT, L. L. REGEL, G. V. SARAFANOV, M. HAMIDI, I. V. VIDESKII and A. M. TURKANINOV, *ibid.* **79** (1986) 77.
4. G. R. CORIELL and R. F. SEKERKA, *ibid.* **46** (1979) 479.
5. F. R. ZOFRAN and S. L. LEHOCZKY, *ibid.* **70** (1984) 349.
6. K. KINOSHITA and K. SUGII, *ibid.* **71** (1985) 283.
7. T. V. FU and W. R. WILCOX, *ibid.* **48** (1990) 416.
8. C. J. CHANG and W. R. WILCOX, *ibid.* **21** (1974) 135.
9. T. JASINSKI and A. F. WITT, *ibid.* **71** (1985) 295.
10. C. A. WANG, A. F. WITT and J. R. CARRUTHERS, *ibid.* **66** (1984) 299.
11. F. M. CARLSON, A. L. FRIPP and R. K. CROUCH, *ibid.* **68** (1984) 747.
12. P. M. ADORNATO and R. A. BROWN, *ibid.* **80** (1987) 195.
13. C. J. CHANG and R. A. BROWN, *ibid.* **63** (1983) 343.
14. C. L. JONES, P. CAPPER, J. J. GOSNEY and I. KENWORTHY, *ibid.* **69** (1984) 281.
15. P. G. BARBER, R. F. BERRY, W. J. DEBNAM, A. L. FRIPP, YU. HUANG and K. STACY, *ibid.* **97** (1989) 672.
16. P. CAPPER, J. J. GOSNEY, C. L. JONES and M. J. T. QUELCH, *ibid.* **63** (1983) 154.
17. A. F. WITT, H. C. GATOS and M. LICHTENSTEIGER, *J. Electrochem. Soc.* **125** (1978) 1832.
18. D. E. HOLMES and H. C. GATOS, *ibid.* **125** (1978) 1873.
19. YU. HUANG, W. J. DEBNAM and A. L. FRIPP, *J. Crystal Growth* **104** (1990) 315.
20. L. Y. CHIN and F. M. CARLSON, *ibid.* **62** (1983) 561.
21. T. JASINSKI, A. F. WITT and W. M. ROHSENOW, *ibid.* **67** (1984) 173.
22. R. J. NAUMAN and S. L. LEHOCZKY, *ibid.* **61** (1983) 707.
23. P. CAPPER, W. G. COATES, C. L. JONES, J. J. GOSNEY, C. K. ARD and I. KENWORTHY, *ibid.* **83** (1987) 69.
24. A. L. FRIPP, R. K. CROUCH, W. J. DEBNAM and I. O. CLARK, *ibid.* **73** (1985) 304.
25. V. FANO, R. PERGOLARI and L. ZANOTTI, *J. Mater. Sci* **14** (1979) 535.
26. J. S. TURNER, in "Buoyancy effects in fluids", edited by G. K. Batchelor and J. W. Miles (Cambridge University Press, Cambridge, 1979) p. 285.

Received 25 July 1996
and accepted 24 July 1997